Progress In Electromagnetics Research M, Vol. 93, 155–164, 2020

Design and Analysis of a Microstrip Planar UWB Bandpass Filter with Triple Notch Bands for WiMAX, WLAN, and X-Band Satellite Communication Systems

Abdul Basit[1, *], Muhammad I. Khattak[1], and Mu'ath Al-Hasan[2]

Abstract—This manuscript presents a UWB filter with three notch bands for WiMAX, WLAN, and X-Band Satellite Communication by introducing inverted E- and T-shape resonators shorted at the center, designed and fabricated for the use of UWB applications authorized by the US Federal Communications Commission. First, a UWB filter ranges from 2.8 GHz to 10.6 GHz is designed by employing four $\lambda/4$ wavelength short-circuited stubs and then couples E- and T-shape resonators on either side of the main transmission line of the proposed UWB filter to achieve notch bands response centered at the resonance frequency of 3.3 GHz for WiMAX applications, 5.1 GHz for WLAN wireless applications, and 8.3 GHz for X-band satellite communication systems, respectively. The proposed filter is able to produce three individually control stopband frequencies centered at 3.3 GHz, 5.1 GHz, and 8.3 GHz with minimum attenuation levels of −28 dB, −19 dB, and −15 dB, respectively. This indicates that the presented filter can efficiently reject superfluous bands at 3.3 GHz in WiMAX system, 5.1 GHz in WLAN system, and 8.3 GHz in satellite communication systems to improve the performance of the UWB communication systems. Finally, the proposed filter with circuit area 34 mm × 12 mm × 0.762 mm is designed and fabricated. A reasonable agreement can be seen between the simulated and fabricated measurements.

1. INTRODUCTION

The frequency spectrum ranges from 3.1 GHz to 10.6 GHz with a centre frequency of 6.825 GHz, and a bandwidth of 7.5 GHz is called ultra-wideband (UWB). In 2002, the FCC (US-Federal Communication Commission), a government organization for frequency bands allocation, authorized the frequency band for UWB applications for commercial purposes such as tracking, medical imaging and position location, vehicular radar systems, communication and measurement systems, military defence purposes, etc. [1, 2]. Since then, much research has been going in this field in both industry and academia. Due to their advantages of low cost, small size, a high data rate of 100 Mbps to 1 Gbps, ease of integration with low power and high-speed communication devices, and low power consumption, UWB microstrip planar filters gain much attention [3]. Meanwhile, it is very important to design a UWB BPF (bandpass filter) with stopbands that suppress the superfluous wireless frequency bands which may affect the FCC UWB range such as WiFi (2.4 GHz), WiMAX IEEE 802.16 (3.3 GHz to 3.6 GHz), IEEE 802.11a lower bands (5.15 GHz to 5.35 GHz), and 8 GHz for XSCS (X-band satellite communication systems). Previously diverse methods have been described to accomplish a UWB filter with stopband characteristics. For instance, a UWB filter was realized by the authors of [4–10] using SIR (step impedance resonator), ASIR (asymmetric stepped impedance resonator), MMRs (multimode resonators), and DGS (defected ground structure). In [4], a filter with wide bandwidth is designed using SIR to control the spurious

Received 26 April 2020, Accepted 12 June 2020, Scheduled 24 June 2020
* Corresponding author: Abdul Basit (abdulbasit@uetpeshawar.edu.pk).
[1] Department of Electrical Engineering, University of Engineering and Technology Peshawar, Pakistan. [2] College of Engineering, Al Ain University, UAE.

bands, but the proposed method suffers from greatly the circuit complexity and the resonator analysis. Another state of the art UWB BPF with wide stopband and high selectivity is demonstrated in [5] using ASIR, but the circuit complexity was a major drawback associated with the design. The authors of [6] designed a UWB filter based on MMR with good in-band performance, but the larger circuit dimension and high insertion loss were the major drawbacks associated with the design. A UWB filter with compact size based on DGS was designed and implemented in [7, 8], but due to the DGS technique, the signal integrity is destroyed. A filter based on rectangular stubs and split circular rings was designed by the authors of [9], but the bandwidth of the reported filter was not large enough. A filter with wide bandwidth is proposed in [10], using the technique of multi-layer structure; however, the circuit complexity and difficult design procedure were the major drawbacks associated with the design. UWB filters with low insertion loss have been realized in [11–13], using cascading lowpass and high pass topology, and the filters based on stub-loaded multimode resonators are implemented in [14–21]. UWB filters with stopband characteristic have been studied through various methods such as SIR [22, 23] and MMRs [24], but the reported designs have large circuit dimensions. To overcome the circuit dimension problem, the authors of [25–28] designed UWB notch filters based on DGS and DMS (defected microstrip structures) techniques, but it is difficult to attain sharp selectivity and wide bandwidth. However, it is still a difficult job for microwave researcher to design a UWB bandpass filter with notch bands having a simple topology and design procedure and good wideband, simultaneously.

The major aim of this research work is to design and fabricate a UWB BPF with a simple topology that passes the proposed frequency range set by FCC with low insertion loss and rejects the undesired signals that may interfere in the given range. First, a UWB BPF is designed using four-quarter wavelength short-circuited stubs which improve the edge steepness of the passband and overall performance of the filter. Then, E- and T-shaped resonators with centrally loaded short-circuited stubs are integrated into the initial UWB filter to achieve the dual- and tri-notch bands response centred at 3.3 GHz, 5.1 GHz, and 8.3 GHz for WiMAX, WLAN, and XSCS applications. To verify the design concept, the proposed samples are fabricated on a Rogers RO-4350 substrate material having a dissipation factor $\delta = 0.004$, height $h = 0.762$ mm, and relative permittivity $\varepsilon_r = 3.66$, respectively.

2. BASIC UWB FILTER AND E-SHAPED RESONATOR ANALYSIS

The basic ultra-wideband circuit configuration without E- and T-shaped resonators together with its corresponding S-parameter frequency plot is depicted in Fig. 1, while the design method of the dual- and tri-notch filters is demonstrated in Fig. 2. The proposed UWB filter comprises four quarter wavelength short-circuited stubs which improve the edge steepness of the passband and overall performance of the filter. The S-parameter frequency plot shows that the proposed filter has a good passband property in the given range set by the FCC. The filter also has good fractional bandwidth of 116%, high reflection loss better than −15 dB, and low insertion loss of 0.4 dB from 2.8 GHz to 7.9 GHz and 0.8 dB from 7.9 GHz to 10.6 GHz, respectively.

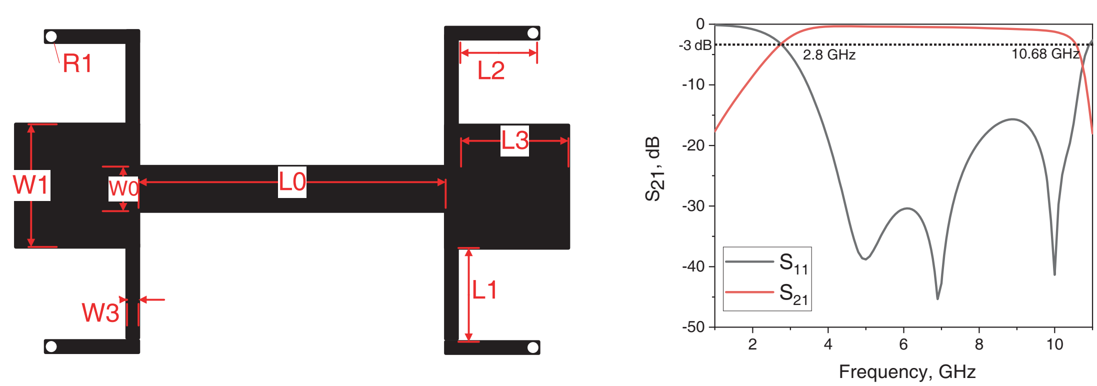

(a) (b)

Figure 1. (a) UWB filter together with its (b) S-parameter frequency plot.

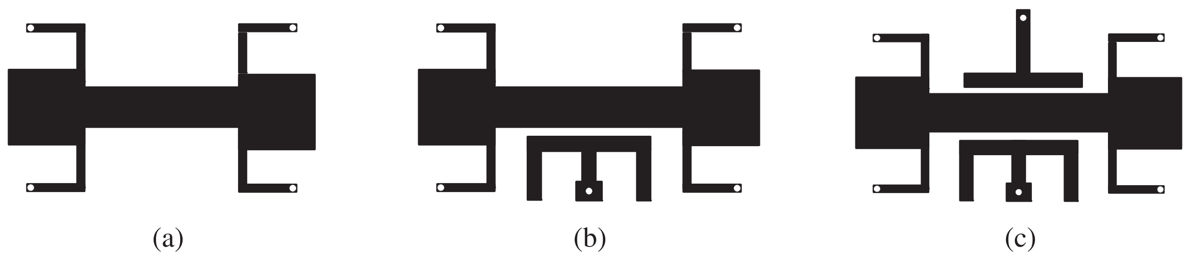

Figure 2. (a) UWB filter without E and T-shaped structure. (b) Dual stopband filter without T-shaped resonator. (c) Tri notch UWB filter including E- and T-shaped resonators.

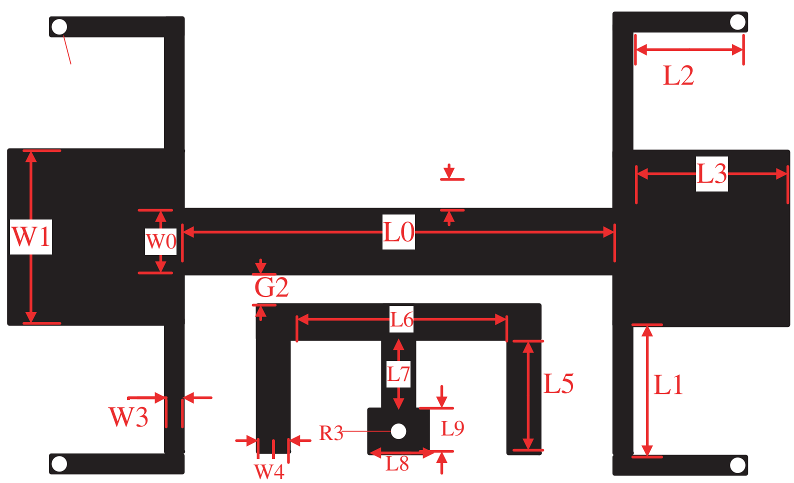

Figure 3. Dual-notch filter configuration.

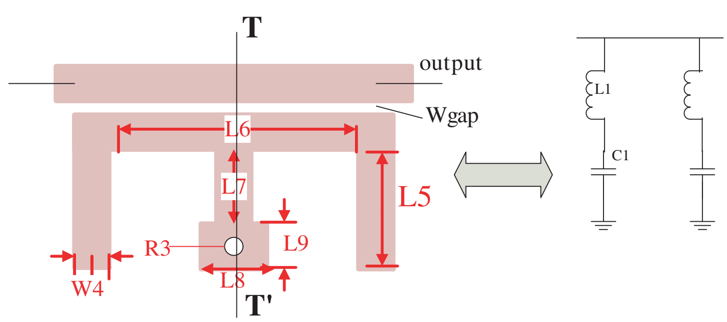

Figure 4. The E-shaped model with its equivalent circuit.

Figure 3 illustrates the topology of the proposed dual-notch UWB filter. The proposed topology is implemented using an E-shaped step impedance hairpin resonator coupled to the initial UWB filter [33]. The basic model of the shorted E-shaped resonator together with its equivalent circuit configuration is depicted in Fig. 4. The proposed layout is symmetrical; therefore, even-odd analysis technique is useful to realize the stopband characteristic. The electrical field dispersal for the even-odd mode is illustrated in Fig. 5. At the plane TT′, the distribution of current is symmetrical for the even mode and anti-symmetrical for the odd mode. Based on this distribution, the fundamental resonance frequencies for the even-odd mode notch bands can be expressed by the method discussed in [34], which is given below;

$$F_{\textit{even-notch}} = \frac{c}{\lambda_{\textit{even-notch}}\sqrt{\varepsilon_{\textit{eff}}}} = \frac{c}{4(L_5 + L_{6/2} + L_7)\sqrt{\varepsilon_{\textit{eff}}}} \tag{1}$$

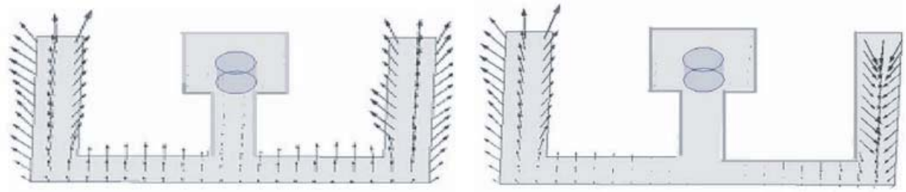

Figure 5. Even and odd mode electrical field distributions.

$$F_{odd\text{-}notch} = \frac{c}{\lambda_{odd\text{-}notch}\sqrt{\varepsilon_{eff}}} = \frac{c}{4(L_5 + L_{6/2})\sqrt{\varepsilon_{eff}}} \quad (2)$$

where $f_{even\text{-}notch}$, $f_{odd\text{-}notch}$, $\lambda_{even\text{-}notch}$, and $\lambda_{odd\text{-}notch}$ indicate the notch band resonance frequencies of the even and odd modes and the corresponding wavelengths, and c indicates the velocity of electromagnetic light. ε_{eff} indicates the effective permittivity of the Roger RO-4350 substrate.

3. T-SHAPED RESONATOR ANALYSIS

The aforementioned idea of the dual-notch band can be extended to implement the tri-notch band UWB filter. For this, an inverted T-shaped resonator is coupled to the dual-notch band UWB filter to get the triple notch response at a frequency of 3.3 GHz [36]. Fig. 6(a) illustrates the basic structural model of the shorted T-shaped resonator. The proposed structure is symmetric along AA′, so again odd-even mode analysis technique is applied to find out the central frequency. Fig. 6(b) shows the odd mode equivalent circuit while Fig. 6(c) illustrates the equivalent circuit of even-mode of the shorted T-shaped resonator. Therefore, the characteristic input impedances of the even-odd-mode can be stated as

$$Z_{in,even} = jZ_{10}\frac{Z_{10}\tan\theta_{10} + 2Z_4\tan\theta_4}{Z_{10} - 2Z_4\tan\theta_{10}\tan\theta_4} \quad (3)$$

$$Z_{in,odd} = jZ_{10}\tan\theta_{10} \text{ where } \theta_{10} = \beta L_{10/2},\ \theta_4 = \beta L_4 \quad (4)$$

where Z_4, Z_{10} indicate the characteristic impedances, and θ_4, θ_{10} indicate the electrical lengths of the open and short-circuited stubs. The fundamental resonance frequencies f_{even} and f_{odd} can be calculated using the procedure discussed in [35] and are given in Eqs. (5) and (7). It should be noted that for passbands the two signals must be in phase, but here the two signals are out of phase to form the stopband.

$$F_{odd\text{-}notch1} = \frac{c}{4(L_{10/2})\sqrt{\varepsilon_{eff}}} = \frac{c}{2(L_{10})\sqrt{\varepsilon_{eff}}} \quad (5)$$

$$F_{even\text{-}notch1} = \frac{c}{4(L_{10/2} + L_4)\sqrt{\varepsilon_{eff}}} \quad (6)$$

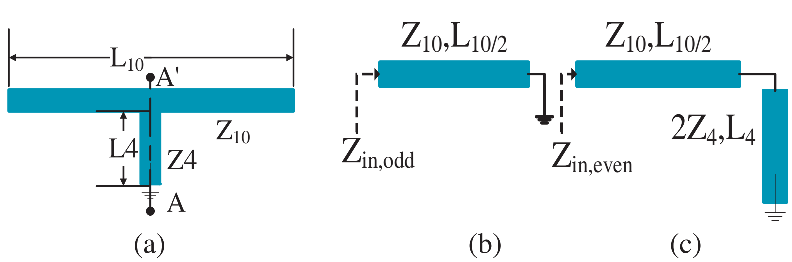

Figure 6. (a) Proposed layout of shorted T-shaped structure. (b) The equivalent circuit of odd mode and (c) even mode.

For simplicity, f_{even} can also be calculated by assuming $L_{10} = 2L_4$. Therefore, the above equation can also be written;

$$F_{even\text{-}notch1} = \frac{c}{4(L_{10/2} + L_{10/2})\sqrt{\varepsilon_{eff}}} = \frac{c}{4(L_{10})\sqrt{\varepsilon_{eff}}} \quad (7)$$

4. FILTER GEOMETRY

A dual- and tri-notch ultra-wideband bandpass filter is designed as shown in Fig. 7, while its corresponding geometrical dimensions in millimetre (mm) are $L_0 = 15$, $L_1 = 4$, $L_2 = 5.3$, $L_3 = 9.5$, $L_4 = 6$, $L_5 = 4$, $L_6 = 7$, $L_7 = 1.21$, $L_8 = L_9 = 1.6$, $L_{10} = 11$, $W_0 = 1.7$, $W_1 = 3$, $W_2 = W_3 = 0.3$, $W_4 = 0.6$, $W_5 = 0.3$, $G_1 = G_2 = 0.1$, $R_1 = 0.3$, $R_2 = 0.24$, and $R_3 = 0.6$, respectively. Two and three independently controlled notches are realized using inverted E and T shaped shorted resonators. The filter can efficiently suppress superfluous bands in the WiMAX system at 3.3 GHz, 5.1 GHz in the WLAN system, and 8.3 GHz in the XSC system. The proposed filter is designed in 3D electromagnetic simulator software HFSS 13.0. The overall area of the filter is 34 mm × 12 mm $(0.06\lambda_g \times 0.02\lambda_g)$, where λ_g shows the wavelength of a guided medium at 3.3 GHz and is tested on Agilent E5071C Network Analyzer.

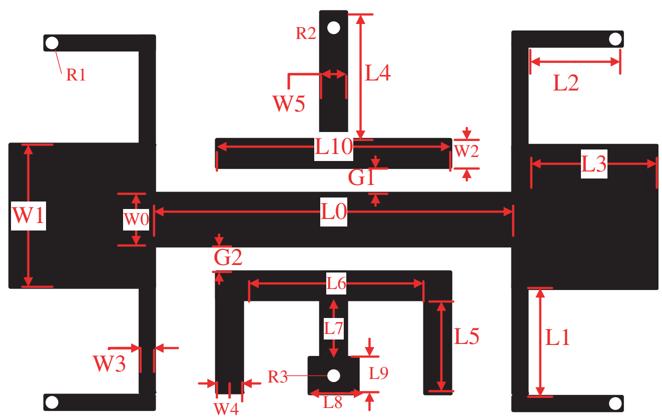

Figure 7. Tri notch UWB filter.

5. RESULTS AND DISCUSSION

In this manuscript, dual and triple notched bands UWB BPFs centred at 3.3 GHz (WiMAX), 5.1 GHz (WLAN), and 8.3 GHz (XSCS) are designed and fabricated. The control of each stopband is investigated according to the following manner. First, the parametric analysis of dual-notch UWB filter is performed independently using only an E-shaped resonator, and then tri-notch band filter analysis is considered by adding shorted T-shaped resonator to the dual-notch UWB filter. The first and second stopbands of the dual-notch E-shaped resonator are created through fundamental even-odd-mode technique and by varying the stub length L_7 from 0.6 mm to 1.2 mm will shift down only the lower notch band according to Eq. (1), while the second notch remains unchanged as shown in Fig. 8. According to Eq. (2), the lower and upper notch bands will move down simultaneously by varying the parametric values of L_5 and L_6, respectively, as shown in Figs. 9 and 10. Therefore, it is confirmed from the frequency plots that to get the desired stopband frequencies, $f_{notch\text{-}odd}$ can be obtained by tuning the parametric values of L_5 and L_6 while $f_{notch\text{-}even}$ can be controlled simply by stub length L_7. It should be noted that by decreasing the gap G_2, the rejection level of the notch bands will increase, and thus stopband performance of the filter will improve.

The first stopband of the triple notch UWB filter is created through a fundamental even-odd-mode method of the shorted T-shaped resonator. It is clearly expressed in Eqs. (5) and (7) that both even-odd-mode fundamental resonance frequencies are controlled through the stub length L_{10} under the condition

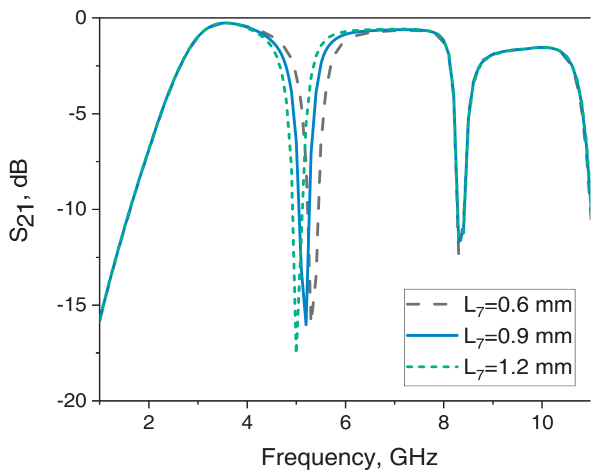

Figure 8. S_{21} plot of dual-notch filter with different L_7.

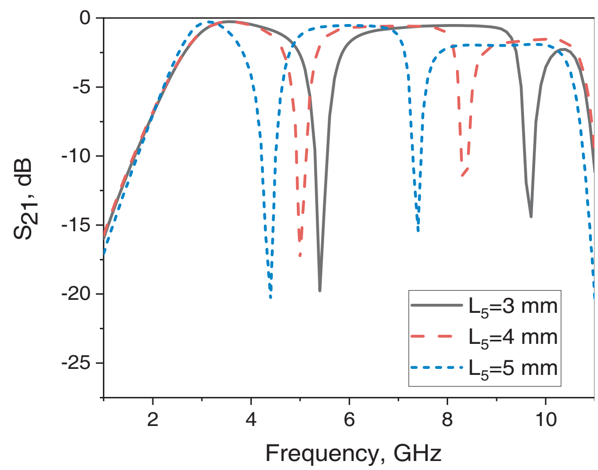

Figure 9. S_{21} results of dual-notch filter against L_5.

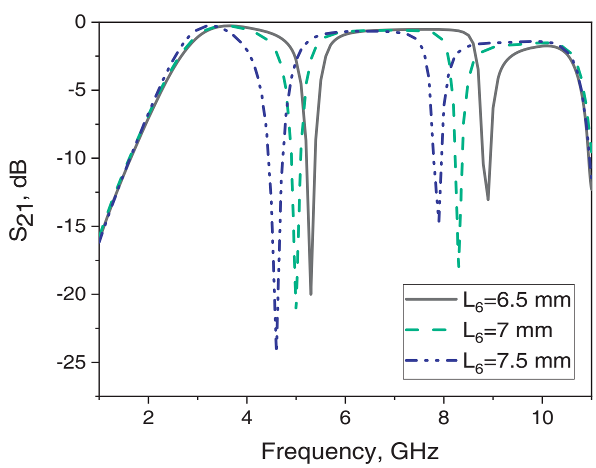

Figure 10. S_{21} plot of dual-notch filter against L_7.

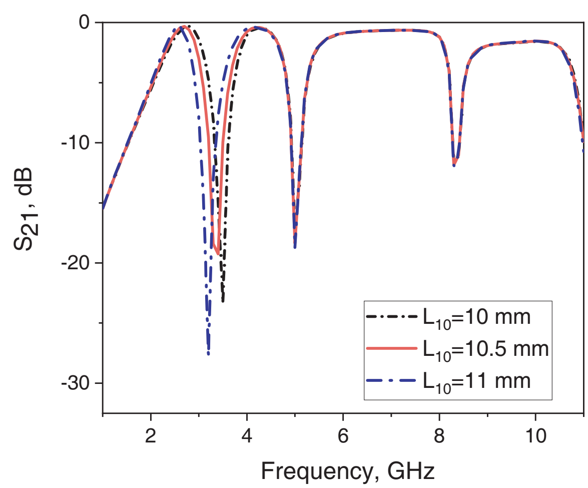

Figure 11. S_{21} plot of tri notch filter against L_{10}.

of $L_{10} = 2L_4$, and varying L_{10} from 10 mm to 11 mm will move down only the resonance frequency of the first stopband while keeping the remaining bands unchanged as shown in Fig. 11. Fig. 12 shows that when W_2 is decreased from 0.6 mm to 0.4 mm, the first stopband also decreases from 3.2 to 3 GHz, while keeping the remaining bands unchanged. The first even mode resonance frequency can also be controlled through length L_4 according to Eq. (6), and increasing L_4 from 5 mm to 6 mm will tune down only the first stopband with no effect on other bands as shown in Fig. 13. The control of the second stopband of the proposed triple notch UWB filter is described in Fig. 14, and increasing the length L_7 will tune down only the second resonance frequency while keeping the third band constant. A very small effect in the first stopband can be seen. Using Eq. (2), when the length L_6 is varied from 7.1 mm to 8.1 mm, both the second and third bands are tuned down simultaneously with negligible effect on the first band as depicted in Fig. 15. Therefore, it is confirmed from the above discussion that all the fundamental resonance frequencies of the proposed tri-notch UWB filter can be varied independently by the stub length of the loaded resonators.

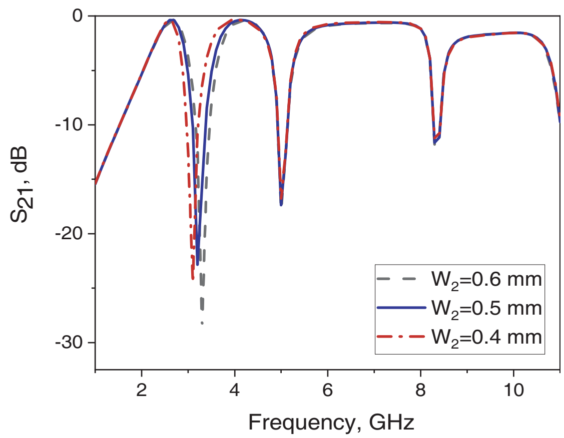

Figure 12. S_{21} plots of triple notch filter against W_2.

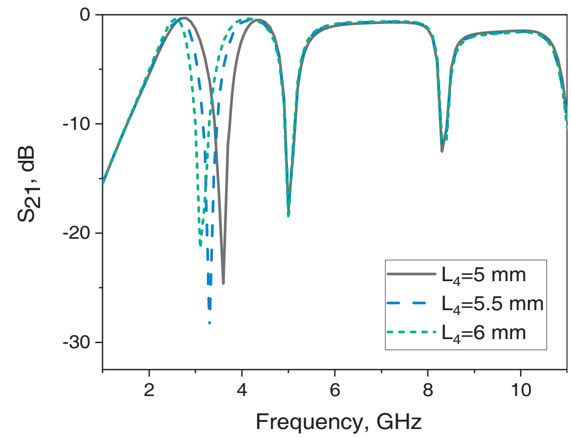

Figure 13. S_{21} results of triple notch filter against L_4.

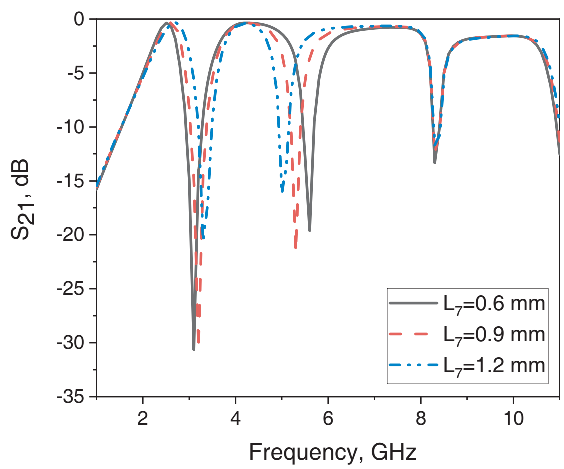

Figure 14. S_{21} plots of tri notch filter with different L_7.

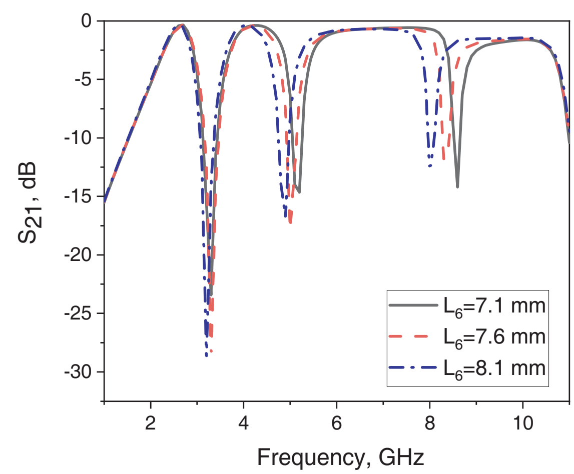

Figure 15. S_{21} plots of tri notch filter against L_6.

6. EXPERIMENTAL AND MEASURED RESULTS

The UWB bandpass filter along with double and triple notch bands is successfully designed and tested using vector network analyser Agilent E5071C. A good match can be realised in both measured and simulated results. First, a UWB filter is designed in the range of 2.8 to 10.6 GHz with a fractional bandwidth 116%, a bandwidth of 7.8 GHz, and the lowest possible insertion losses of 0.4 dB from 2.8 GHz to 7.9 GHz and 0.8 dB from 7.9 GHz to 10.6 GHz, respectively. The designed filter has a total area of 34 mm × 12 mm ($0.06\lambda_g \times 0.02\lambda_g$). After that, a dual-notch band centred at 5.1 GHz and 8.3 GHz is designed for WLAN and XSCS applications, with the lowest possible rejection levels of −19 dB and −15 dB, respectively. Fig. 16 shows the photograph and S-parameter plots of both simulated and experimental results of the dual-notch filter. Finally, a triple notch UWB filter for WiMAX application is designed by adding a shorted T-shaped resonator to the initial dual-notch filter with a stopband frequency centred at 3.3 GHz. The attenuation level of the proposed triple notch filter is −28 dB, −19 dB, and −15 dB for the first, second, and third stopbands, respectively. The corresponding absolute fractional bandwidths for lower, middle, and upper-frequency notch bands are 24.24%, 12.06%, and 7.8%. Fig. 17 shows the photograph and S-parameter plots of both simulated and experimental results of the triple notch filter. Moreover, the comparison of this research work with some recently published literature is shown in Table 1.

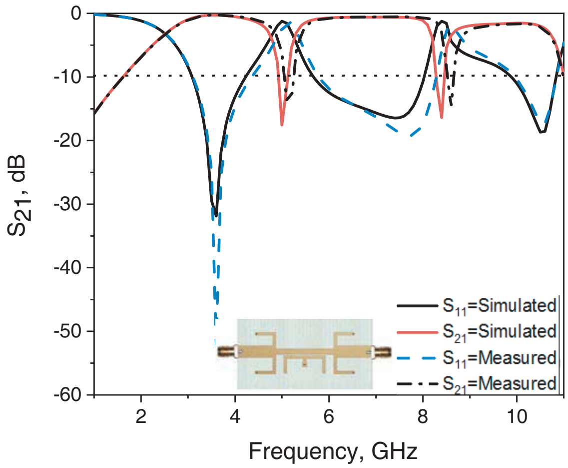

Figure 16. The S-parameter frequency plots of the dual-notch UWB filter.

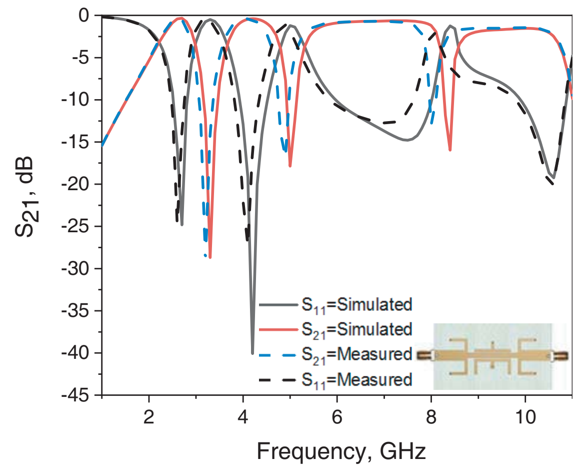

Figure 17. The S-parameter frequency plots of the tri notch UWB filter.

Table 1. Comparison with previous research work.

Serail No.	No. of Stopbands	3 dB FBW (%)	Wide Stopband	S_{11}, S_{21} (dB)	Circuit size ($\lambda_g \times \lambda_g$)
[8]	1	100	No	12, 1.2	NA
[9]	0	80	No	13, 0.35	0.53×0.43
[10]	1	100	Yes	15, 2	0.74×0.42
[29]	0	110	Yes	13, 0.2	0.15×0.12
[30]	0	45	No	14, 1.4	0.3×0.1
[31]	2	107	No	11.7, 2.1	0.89×0.46
[32]	1	100	Yes	10, 2	0.7×0.28
This work	3	116	Yes	> 15, 0.8	0.06×0.02

7. CONCLUSIONS

A new microstrip UWB filter with a bandwidth of 7.8 GHz (excluding the stopbands) and fractional bandwidth of 116% has been designed and fabricated in this paper. To isolate the proposed filter from the mutual interference with WiMAX-IEEE 802.16 (3.3 GHz to 3.6 GHz), WLAN (5.15 GHz to 5.35 GHz), and 8 GHz for XSCS, three notch bands are incorporated centered at 3.3 GHz, 5.1 GHz, and 8.3 GHz with minimum attenuation levels of -28 dB, -19 dB, and -15 dB for the first, second, and third stopbands, respectively. The stopband characteristics in the proposed filter are introduced through symmetric E- and T-shape resonators loaded with a short-circuited stub at the middle. The corresponding absolute fractional bandwidth for the lower, middle, and upper-frequency notch bands are 24.24%, 12.06%, and 7.8%, respectively. Experimental results show a close similarity with the simulations authenticating the performance of the proposed filter.

ACKNOWLEDGMENT

This work is supported by the ADEK Award for Research Excellence (AARE19-245) 2019.

REFERENCES

1. FCC, "Revision of part 15 of the commission's rules regarding ultra-wideband transmission systems," Tech. Rep. ETDocket 98–153, FCC02-48, Federal Communications Commission, Apr. 2002.
2. Chen, F. C. and W. C. Chew, "Time-domain ultra-wideband microwave imaging radar system," *Journal of Electromagnetic Waves and Applications*, Vol. 17, No. 2, 313–331, 2003.
3. George, T. and B. Lethakumary, "High frequency rejection using L shaped defected microstrip structure in ultra wideband bandpass filter," *Materials Today: Proceedings*, Vol. 25, Part 2, 265–268, Feb. 8, 2020.
4. Hung, C. Y., M. H. Weng, and Y. K. Su, "Design of compact and sharp rejection UWB BPFs using interdigital stepped-impedance resonators," *IEICE Electron. Lett.*, Vol. 90, 1652–1654, 2007.
5. Chang, Y. C., C. H. Kao, M. H. Weng, and R. Y. Yang, "Design of the compact wideband bandpass filter with low loss, high selectivity and wide stopband," *IEEE Microw. Wirel. Compon. Lett.*, Vol. 18, 187–189, 2008.
6. Wong, S. W. and L. Zhu, "Implementation of compact UWB bandpass filter with a notch-band," *IEEE Microw. Wirel. Compon. Lett.*, Vol. 18, 10–12, 2008.
7. Song, Y., G. M. Yang, and W. Geyi, "Compact UWB bandpass filter with dual notched bands using defected ground structures," *IEEE Microw. Wirel. Compon. Lett.*, Vol. 24, 230–232, 2014.
8. Liu, J., W. Ding, J. Chen, and A. Zhang, "New ultra-wideband filter with sharp notched band using defected ground structure," *Progress In Electromagnetics Research Letters*, Vol. 83, 99–105, 2019.
9. Choudhary, D. K. and R. K. Chaudhary, "A compact via-less metamaterial wideband bandpass filter using split circular rings and rectangular stub," *Progress In Electromagnetics Research Letters*, Vol. 72, 99–106, 2018.
10. Ji, X.-C., W.-S. Ji, L.-Y. Feng, Y.-Y. Tong, and Z.-Y. Zhang, "Design of a novel multi-layer wideband bandpass filter with a notched band," *Progress In Electromagnetics Research Letters*, Vol. 82, 9–16, 2019.
11. Hsu, C. L., F. C. Hsu, and J. K. Kuo, "Microstrip bandpass filters for ultra-wideband (UWB) wireless communications," *IEEE MTT-S International Microwave Symposium Digest*, 4, 682, IEEE, 2005.
12. Yang, G. M., et al., "Design of ultra-wide band (UWB) bandpass filter based on defected ground structure," *Microwave and Optical Technology Letters*, Vol. 49, No. 6, 1374–1377, 2010.
13. Wu, C. H., et al., "A compact LTCC ultra-wideband bandpass filter using semi-lumped parallel-resonance circuits for spurious suppression," *2007 European Microwave Conference*, 532–535, Munich, 2007.
14. Hong, J.-S. and H. Shaman, "An optimum ultra-wideband microstrip filter," *Microwave and Optical Technology Letters*, Vol. 47, No. 3, 230–233, 2010.
15. Wong, W. T., et al., "Highly selective microstrip bandpass filters for ultra-wideband (UWB) applications," *2005 Asia-Pacific Microwave Conference Proceedings*, 4, IEEE, 2005.
16. Shaman, H. and J. S. Hong, "A novel ultra-wideband (UWB) bandpass filter (BPF) with pairs of transmission zeroes," *IEEE Microw. Wirel. Compon. Lett.*, Vol. 17, No. 2, 121–123, 2007.
17. Shaman, H. and J. S. Hong, "An optimum ultra-wideband (UWB) bandpass filter with spurious response suppression," *2006 IEEE Annual Wireless and Microwave Technology Conference*, 1–5, Clearwater Beach, FL, 2006.
18. Deng, H. W., et al., "Compact quintuple-mode stub-loaded resonator and UWB filter," *IEEE Microw. Wirel. Compon. Lett.*, Vol. 20, No. 8, 438–440, 2010.
19. Zhu, H. and Q. X. Chu, "Compact ultra-wideband (UWB) bandpass filter using dual-stub-loaded resonator (DSLR)," *IEEE Microw. Wirel. Compon. Lett.*, Vol. 23, No. 10, 527–529, 2013.
20. Chu, Q. X., X. H. Wu, and X. K. Tian, "Novel UWB bandpass filter using stub-loaded multiple-mode resonator," *IEEE Microw. Wirel. Compon. Lett.*, Vol. 21, No. 8, 403–405, 2011.

21. Zhu, L., S. Sun, and W. Menzel, "Ultra-wideband (UWB) bandpass filters using multiple-mode resonator," *IEEE Microw. Wirel. Compon. Lett.*, Vol. 15, No. 11, 796–798, 2005.
22. Wei, F., W. T. Li, X. W. Shi, and Q. L. Huang, "Compact UWB bandpass filter with triple-notched bands using triple-mode stepped impedance resonator," *IEEE Microw. Wirel. Compon. Lett.*, Vol. 22, 512–514, 2012.
23. Wei, F., P.-Y. Qin, Y. J. Guo, and X.-W. Shi, "Design of multi-band bandpass filters based on stub loaded stepped-impedance resonator with defected microstrip structure," *IET Microw. Antennas Propag.*, Vol. 10, 230–236, 2016.
24. Lu, X., B. Wei, Z. Xu, B. Cao, X. Zhang, R. Wang, and F. Song, "Superconducting ultra-wideband (UWB) bandpass filter design based on quintuple/quadruple/triple-mode resonator," *IEEE Trans. Microw. Theory Tech.*, Vol. 63, 1281–1293, 2015.
25. Zhang, C., J. Zhang, and L. Li, "Triple band-notched UWB antenna based on SIR-DGS and fork-shaped stubs," *Electron. Lett.*, Vol. 50, 67–69, 2014.
26. Zhou, L.-H., Y. Ma, J. Shi, J. Chen, and W. Che, "Differential dual-band bandpass filter with tunable lower band using embedded DGS unit for common-mode suppression," *IEEE Trans. Microw. Theory Tech.*, Vol. 64, 4183–4191, 2016.
27. Zakaria, Z., M. A. Mutalib, A. Ismail, M. S. M. Isa, M. M. Ismail, A. A. Latiff, N. A. Zainuddin, and W. Y. Sam, "Compact structure of band-pass filter integrated with Defected Microstrip Structure (DMS) for wideband applications," *Proceedings of the European Conference on Antennas and Propagation*, Vol. 21, 2158–2162, The Hague, The Netherlands, Apr. 6–11, 2014.
28. Wang, J., J. Zhao, and J. L. Li, "Compact UWB bandpass filter with triple notched bands using parallel U-shaped defected microstrip structure," *Electron. Lett.*, Vol. 50, 89–91, 2014.
29. Deng, K. and W. Feng, "Wideband bandpass filter with multiple transmission zeros and compact size," *Microw. Opt. Technol. Lett.*, Vol. 58, 2452–2455, 2016.
30. Zhang, Z.-C. and H. Liu, "A ultra compact wideband bandpass filter using a quadmode stub-loaded resonator," *Progress In Electromagnetics Research Letters*, Vol. 77, 35–40, 2018.
31. Li, Y., W. W. Choi, K. W. Tam, and L. Zhu, "Novel wideband bandpass filter with dual notched bands using stub-loaded resonators," *IEEE Microw. Wirel. Compon. Lett.*, Vol. 27, 25–27, 2017.
32. Weng, M.-H., C.-W. Hsu, S.-W. Lan, and R.-Y. Yang, "An ultra-wideband bandpass filter with a notch band and wide upper bandstop performances," *Electronics*, Vol. 8, No. 11, 1316, 2019.
33. Zheng, X. and T. Jiang, "Design of UWB bandpass filter with dual notched bands using E-shaped resonator," *2016 IEEE/ACES International Conference on Wireless Information Technology and Systems (ICWITS) and Applied Computational Electromagnetics (ACES)*, 1–2, IEEE, 2016.
34. Basit, A. and M, I. Khattak, "Designing modern compact microstrip planar quadband bandpass filter for hand held wireless applications," *Frequenz*, Vol. 74, Nos. 5–6, 219–227, Jan. 4, 2020.
35. Sami, A., M. U. Rahman, and S. Bashir, "Design of compact tri and quad band band-pass filters using stub loaded resonators for wireless applications," *SN Applied Sciences*, Vol. 1, No. 9, 1019, 2019.
36. Basit, A., M. I. Khattak, A. R. Sebak, A. B. Qazi, and A. A. Telba, "Design of a compact microstrip triple independently controlled pass bands filter for GSM, GPS and WiFi applications," *IEEE Access*, Vol. 8, 77156–77163, 2020, doi: 10.1109/ACCESS.2020.2989377.